

Internal energy excitation and dissociation of molecular nitrogen in a compressing flow

By T. E. Magin, M. Panesi[†], A. Bourdon[‡], R. Jaffe AND D. Schwenke

1. Motivation and objective

Prediction of the radiative heat-flux to the surface of a spacecraft entering a planetary atmosphere strongly depends on the completeness and accuracy of the physical model used to describe the non-equilibrium phenomena in the flow. During an atmospheric entry, the translational energy of the fluid particles drastically rises through a shock. Depending on the intensity of the shock, different physico-chemical processes may take place, such as excitation of the internal energy modes, dissociation of the molecules, ionization of the atoms and molecules. These non-equilibrium phenomena are strongly coupled to each other. For re-entry velocities >10 km/s, a significant portion of the heating experienced by the heat shield can be due to radiation and is highly influenced by the shape of the internal energy distribution function. Understanding thermo-chemical non-equilibrium effects is also important for a correct interpretation of experimental measurements in flight and in ground wind-tunnels. Concentration of the gas species and distribution of their internal energy level populations can be estimated by means of either multi-temperature models (Park 1990) or collisional radiative (CR) models (Laux 2002; Bultel *et al.* 2006; Magin *et al.* 2006; Panesi *et al.* 2009).

In multi-temperature models, the physico-chemical properties of the air flow are obtained by assuming that, for all the species, the population of each internal energy mode follows a Boltzmann distribution at its own temperature (T_r rotational, T_v vibrational or T_e electronic temperature, respectively). These models have been developed based on experimental data obtained in flight and also in high-enthalpy facilities representative of specific flight conditions, such as in arc-jet and shock-tube wind-tunnels (Appleton *et al.* 1968). The problem with this approach is that the models may contain many uncertainties that can be extremely difficult to quantify. Moreover, there is no detailed information about the specific state of the gas since these data are highly averaged (e.g., stagnation point heat-flux measurement). Park (2006) has worked extensively on multi-temperature models for air and has also shown that the use of these models, even if very efficient from a computational point of view, can be justified only when the departure from the Boltzmann population is small, i.e., for low-velocity and high-pressure re-entry conditions.

Collisional radiative models take into account all relevant collisional and radiative mechanisms between the internal energy levels of the different species in the flow. They constitute a valid alternative to the multi-temperature models since they exhibit a wider range of applicability. By increasing order of complexity and computational time, three kinds of CR models can be distinguished for air: *electronic*, *vibrational* and *rovibrational*. In electronic CR models, transitions between the electronic states are considered and the rovibrational levels of the molecules are populated according to Boltzmann distributions

[†] Institute for Computational Engineering and Sciences, The University of Texas at Austin

[‡] Laboratoire EM2C – UPR 288 CNRS, Ecole Centrale Paris, France

at temperatures T_r and T_v . In vibrational CR models, transitions between the vibrational states of the molecules are also considered and only a rotational temperature T_r is defined. Finally, in rovibrational CR models, no temperature is required to describe the internal energy. The quality of the results obtained with a CR model relies mainly on the accuracy of the rate coefficients for elementary processes between energy levels. Different theoretical models have been developed in the literature to determine elementary rate coefficients: for instance, the quasiclassical trajectory method using a potential energy surface which is a fit to *ab initio* electronic structure calculations (Schwenke 1990), the same method based on approximate energy surfaces (Esposito *et al.* 2006) and analytical models such as the forced harmonic oscillator (Macheret & Adamovich 2000). Recently, the computational chemists at NASA Ames Research Center have embarked on the characterization of non-equilibrium air chemistry from first principles (Chaban *et al.* 2008; Jaffe *et al.* 2008, 2009). So far, the $N_2 + N$ system has been studied to yield rate coefficients and cross-sections for rovibrational excitation and dissociation of molecular nitrogen in the ground electronic state. First principle quantum chemistry calculations are used to generate realistic nuclear interaction potentials. The quasiclassical trajectory method is then used to yield the fundamental data required for a rigorous treatment of non-equilibrium chemistry.

The present work is at the interface between computational chemistry and computational fluid dynamics and aims at developing new models based on microscopic theory and applying them to macroscopic scale. The database recently developed at NASA Ames Research Center was used to derive vibrational dissociation and excitation rate coefficients for molecular nitrogen (Bourdon *et al.* 2008). In this work, we propose to develop a 1D vibrational CR model to simulate a shock in a nitrogen flow. This model, so far only collisional, is the first component of a larger model for air that will eventually include radiation. It is important to mention that multi-quantum jumps are taken into account for the excitation mechanism. The free stream conditions are carefully selected to stay in the validity range of a simplified mechanism for the $N_2 + N$ system comprising dissociation and vibrational-translational (VT) relaxation. Finally, we compare the results obtained by means of the vibrational CR model to a multi-temperature model often used in the aerospace community.

2. Physico-chemical model

2.1. Energy levels

The NASA Ames database (Schwenke 2008) comprises 9390 (v, J) rovibrational levels for the electronic ground-state of nitrogen, where index v stands for the vibrational quantum number, and index J , the rotational quantum number. These levels can also be denoted by means of a global index i . The relation between the i and (v, J) notations is expressed as follows

$$i = i(v, J), \quad v = 0, \dots, v_{\max}, \quad J = 0, \dots, J_{\max}(v).$$

Conversely, the relation between the (v, J) and i notations is given by the relations

$$v = v(i), \quad J = J(i), \quad i \in I_{\text{BP}},$$

where I_{BP} is the set of global indices for the nitrogen energy levels. Most of these levels are truly bound, *i.e.*, their energy is lower than the dissociation energy relative to the level $(v = 0, J = 0)$, equal to 9.75 eV for the electronic ground-state of nitrogen, while some of the energy levels are predissociated, *i.e.*, their energy is higher than the dissociation

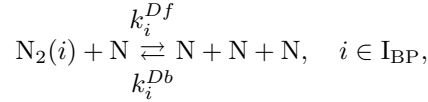
energy relative to the level ($v = 0, J = 0$). The bound energy levels are denoted by the set I_B , and the predissociated energy levels, by the set I_P . The set for all the levels is then given by $I_{BP} = I_B \cup I_P$. The total wave function for the nitrogen molecule must be symmetric with respect to exchanging the nuclei (Bose-Einstein statistics), and thus the degeneracy of the energy levels is given by the expression

$$g_i = (2J(i) + 1)g_i^{NS}, \quad i \in I_{BP},$$

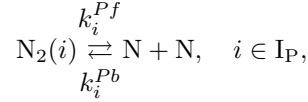
where the nuclear spin degeneracy is

$$g_i^{NS} = \begin{cases} 6: & \text{even } J(i), \\ 3: & \text{odd } J(i). \end{cases}$$

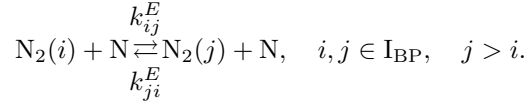
The database for the $N_2 + N$ system comprises more than 23 million reactions, for dissociation of truly bound states and predissociated states,



for predissociation of the predissociated states,



and for excitation between all states,



The direct reaction rate coefficients k_i^{Df} , k_i^{Pf} and k_{ij}^E , $j > i$ are obtained based on the reaction cross-sections for nine values of the gas translational temperature ($T=7500$; 10,000; 12,500; 15,000; 20,000; 25,000; 30,000; 40,000; and 50,000 K). The reverse reaction rate coefficients k_i^{Db} , k_i^{Pb} and k_{ij}^E , $j < i$ are computed based on microreversibility, only using endothermic rate coefficients, although some exothermic rates were also available:

$$\begin{aligned} k_i^{Db}(T) &= k_i^{Df}(T) \frac{g_i Q_{N_2}^t(T) \exp\left(\frac{-(E_i - 2E_N)}{k_B T}\right)}{[g_N Q_N^t(T)]^2}, \quad i \in I_{BP}, \\ k_i^{Pb}(T) &= k_i^{Pf}(T) \frac{g_i Q_{N_2}^t(T) \exp\left(\frac{-(E_i - 2E_N)}{k_B T}\right)}{[g_N Q_N^t(T)]^2}, \quad i \in I_P, \quad j > i, \\ k_{ji}^E(T) &= k_{ij}^E(T) \frac{g_i \exp\left(\frac{-(E_i - E_j)}{k_B T}\right)}{g_j}, \quad i, j \in I_{BP}, \quad j > i, \end{aligned}$$

where the energy of level i is defined as E_i and the translational partition functions as

$$Q_{N_2}^t(T) = \left(\frac{2\pi k_B m_{N_2} T}{h_P^2} \right)^{3/2}, \quad Q_N^t(T) = \left(\frac{2\pi k_B m_N T}{h_P^2} \right)^{3/2},$$

where symbol k_B stands for Boltzmann's constant, and h_P , Planck's constant. The nitrogen atom degeneracy is given by $g_N = 12$ (nuclear and electronic spin).

2.2. Vibrational collisional radiative model

A 1-D vibrational CR model was developed to describe the energy relaxation and dissociation processes in a nitrogen flow. The 61 vibrational energy levels for N_2 of the NASA Ames database are taken into account in the CR model, as well as all the averaged vibrational rate coefficients for dissociation and excitation for the $N_2 + N$ system. The energy for the rovibrational level $i \in I_{BP}$ is defined based on the vibrational contribution and the relative rotational contribution with respect to the vibrational energy level

$$E_i = \tilde{E}_v + \Delta\tilde{E}(v, J), \quad v = 0, \dots, v_{\max}, \quad J = 0, \dots, J_{\max}(v),$$

with $\tilde{E}_v = E_{i(v,0)}$. The rotational energy level populations are assumed to follow a Boltzmann distribution at the translational temperature

$$\frac{n_i}{\tilde{n}_v} = \frac{1}{\tilde{Q}_v(T)} g_i \exp\left(\frac{-\Delta\tilde{E}(v, J)}{k_B T}\right), \quad i \in I_{BP},$$

where the number density, $\tilde{n}_v = \sum_{J=0}^{J_{\max}(v)} n_i$, and the rotational partition function, $\tilde{Q}_v(T) = \sum_{J=0}^{J_{\max}(v)} g_i \exp[-\Delta\tilde{E}(v, J)/(k_B T)]$, are introduced for the vibrational energy levels $v = 0, \dots, v_{\max}$. The average vibrational rate coefficients for dissociation and excitation are given by the expressions

$$\begin{aligned} \tilde{k}_v^{Df}(T) &= \frac{1}{\tilde{Q}_v(T)} \sum_{J=0}^{J_{\max}(v)} g_i \exp\left(\frac{-\Delta\tilde{E}(v, J)}{k_B T}\right) k_i^{Df}(T), \quad v = 0, \dots, v_{\max}, \\ \tilde{k}_{vv'}^E(T) &= \frac{1}{\tilde{Q}_v(T)} \sum_{J=0}^{J_{\max}(v)} g_i \exp\left(\frac{-\Delta\tilde{E}(v, J)}{k_B T}\right) \sum_{J'=0}^{J_{\max}(v')} k_{ij}^E(T), \quad v, v' = 0, \dots, v_{\max}, \end{aligned}$$

where $j = j(v', J')$. Predissociation is not accounted for. Reverse rate coefficients are computed by means of the following relations

$$\begin{aligned} \frac{\tilde{k}_v^{Db}(T)}{\tilde{k}_v^{Df}(T)} &= \frac{Q_{N_2}^t(T) \tilde{Q}_v(T) \exp\left(\frac{-(\tilde{E}_v - 2E_N)}{k_B T}\right)}{[g_N Q_N^t(T)]^2}, \quad v = 0, \dots, v_{\max}, \\ \frac{\tilde{k}_{vv'}^E(T)}{\tilde{k}_{v'v}^E(T)} &= \frac{\tilde{Q}_v(T) \exp\left(\frac{-(\tilde{E}_v - \tilde{E}_{v'})}{k_B T}\right)}{\tilde{Q}_{v'}(T)}, \quad v, v' = 0, \dots, v_{\max}, \quad v' > v. \end{aligned}$$

In section 3, we will choose suitable free stream conditions for which this simplified mechanism is dominant, neglecting ionization, VV relaxation and electronic excitation. Post-shock conditions are derived from the Rankine-Hugoniot jump relations assuming frozen gas composition and vibrational energy modes. The rotational mode is assumed to be in equilibrium with the translational mode. The downstream flowfield is obtained by solving the following steady Euler conservation equations of mass for the N atoms and

for the vibrational energy levels of N₂ molecule, global momentum and global energy

$$\frac{d}{dx}(n_N u) = \tilde{\omega}_N, \quad (2.1)$$

$$\frac{d}{dx}(\tilde{n}_v u) = \tilde{\omega}_v, \quad v = 0, \dots, v_{\max}, \quad (2.2)$$

$$\frac{d}{dx}(\rho u^2 + p) = 0, \quad (2.3)$$

$$\frac{d}{dx}(\rho u H) = 0. \quad (2.4)$$

The chemical production rates are given by the expressions

$$\begin{aligned} \tilde{\omega}_N &= 2 \sum_{v=0}^{v_{\max}} \tilde{k}_v^{Df}(T) \left[\tilde{n}_v n_N - \frac{\tilde{k}_v^{Db}(T)}{\tilde{k}_v^{Df}(T)} (n_N)^3 \right], \\ \tilde{\omega}_v &= -\tilde{k}_v^{Df}(T) \left[\tilde{n}_v n_N - \frac{\tilde{k}_v^{Db}(T)}{\tilde{k}_v^{Df}(T)} (n_N)^3 \right] - \sum_{v'=0}^{v-1} \tilde{k}_{v'v}^E(T) \left[\frac{\tilde{k}_{vv'}^E(T)}{\tilde{k}_{v'v}^E(T)} \tilde{n}_v n_N - \tilde{n}_{v'} n_N \right] \\ &\quad - \sum_{v'=v+1}^{v_{\max}} \tilde{k}_{vv'}^E(T) \left[\tilde{n}_v n_N - \frac{\tilde{k}_{v'v}^E(T)}{\tilde{k}_{vv'}^E(T)} \tilde{n}_{v'} n_N \right], \end{aligned}$$

for $v = 0, \dots, v_{\max}$. The total enthalpy is given by the expression $H = e_{int} + e_t + \frac{1}{2}u^2 + p/\rho$, with the translational energy $e_t = \frac{3}{2}(\tilde{n}_{N_2} + n_N)k_B T/\rho$, the mass density, $\rho = \tilde{n}_{N_2}m_{N_2} + n_N m_N$, the number density for N₂, $\tilde{n}_{N_2} = \sum_{v=0}^{v_{\max}} \tilde{n}_v$, and the mixture pressure, $p = \frac{2}{3}\rho e_t$. The internal energy reads $\rho e_{int} = m_{N_2} \sum_{v=0}^{v_{\max}} \tilde{n}_v [\tilde{E}_v + \tilde{E}_v^{rot}(T)] + m_N n_N E_N$, with the rotational energy of level v given by $\tilde{E}_v^{rot}(T) = k_B T^2 \partial(\ln \tilde{Q}_v)/\partial T \sim k_B T$.

The conservative system of equations (2.1)-(2.4) is transformed into a system of ordinary differential equations (Magin *et al.* 2006). No additional conservation equation for the vibrational energy is considered, since this quantity is directly computed from the vibrational energy population obtained by means of the CR model

$$e_{vib}(x) = \frac{1}{\tilde{n}_{N_2}} \sum_{v=0}^{v_{\max}} \tilde{n}_v(x) \tilde{E}_v. \quad (2.5)$$

One can also define a vibrational temperature based on the relative population among the first excited vibrational energy level and the ground state, as follows:

$$T_v = \frac{\tilde{E}_1}{k_B \ln \left(\frac{\tilde{n}_0}{\tilde{n}_1} \right)}, \quad (2.6)$$

where \tilde{E}_1 is the energy of the first excited vibrational energy level. The post-shock initial population of vibrational energy levels is assumed to follow a Boltzmann distribution

$$\frac{\tilde{n}_v}{\tilde{n}_{N_2}} = \frac{\tilde{Q}_v(T)}{\tilde{Q}(T, T_v)} \exp \left(\frac{-\tilde{E}_v}{k_B T_v} \right), \quad v = 0, \dots, v_{\max},$$

where the total partition function is given by the expression

$$\tilde{Q}(T, T_v) = \sum_{v'=0}^{v_{\max}} \exp \left(\frac{-\tilde{E}_{v'}}{k_B T_v} \right) \tilde{Q}_{v'}(T),$$

	1	2	3
T [K]	4000	40,876	8915
p [Pa]	40	2157	2472
u [km/s]	9	1.706	0.621
x_N [-]	0.086	0.086	0.999

TABLE 1. Translational temperature, pressure, velocity and nitrogen atom mole fraction for the free stream LTE conditions (1), post-shock non-equilibrium conditions at the shock location (2) and post-shock LTE conditions (3).

with the vibrational temperature T_v equal to the freestream translational temperature.

3. Results

The N_2, N free stream gas mixture is assumed to be in Local Thermodynamic Equilibrium (LTE) at $p=40$ Pa pressure and $T=4000$ K translational temperature (i.e., there is 8.6% mole fraction of N atoms). The free stream temperature does not correspond to flight conditions. A high value of temperature was chosen to have enough nitrogen atoms in the flow, since only the mechanism for the $N + N_2$ system is considered in this work; the free stream and post-shock conditions based on the jump relations are reviewed in Table 1, together with the post-shock LTE conditions. Figure 1 compares the evolution of the rotational-translational temperature and vibrational temperature as a function of the distance from the shock for the multi-temperature model of Park ($T = T_r, T_v = T_{ele} = T_e$) for a 5-species mixture (N, N_2, N^+, N_2^+ and e^-) with standard mechanism and for a 2-species mixture (N and N_2) with simplified mechanism. The standard mechanism comprises all the reactions of dissociation, ionization and VT relaxation frequently used in multi-temperature models (Park 1993). The species electronic energy levels is accounted for when computing the flow enthalpy. The simplified mechanism comprises $N_2 + N$ dissociation and Landau-Teller VT relaxation, based on a Millikan-White-Park relaxation time computed from the $N_2 - N$ interaction only (Park 1993). Both multi-temperature models give very close results, the simplified mechanism is thus dominant for the selected free stream conditions when using a multi-temperature model. In both cases, an overshoot of the vibrational temperature and a slow relaxation to equilibrium are noticed. In the following, we will compare the results obtained by means of the collisional radiative model to those based on the multi-temperature model for the 2-species mixture with simplified mechanism (Appleton *et al.* 1968).

Figure 2 compares the evolution of the pressure and velocity for a fluid particle as a function of the Lagrangian time, starting at $t = 0$ with the shock, for the multi-temperature model (2-species mixture with simplified mechanism, Park reaction rate coefficients) and for the vibrational collisional radiative model presented in section 2. We notice that, as expected, the level of accuracy to describe the nitrogen dissociation has a negligible influence on the pressure of the flow. A more significant influence is observed on the velocity field. Table 2 gives the Lagrangian time for a fluid particle, and the corresponding distance from the shock, for the vibrational CR model.

Figure 3 shows the rotational-translational temperature and vibrational temperature as a function of time for the multi-temperature model and the vibrational CR model. The definition of the vibrational temperature for the CR calculation given in Eq. (2.6) is justified considering that the thermodynamic state of the gas is mostly characterized by the

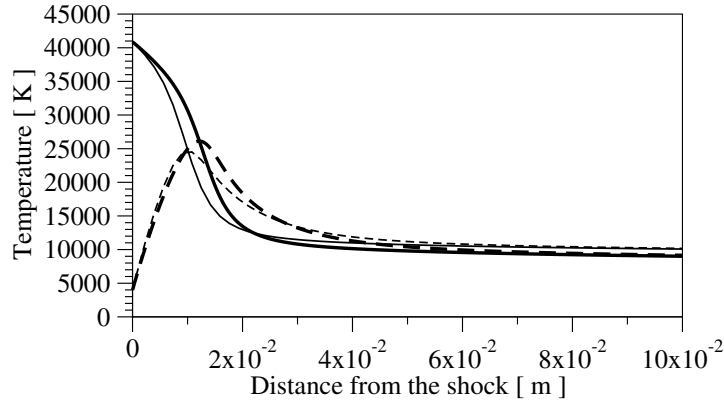


FIGURE 1. Post-shock translational temperature (unbroken lines) and vibrational temperature (dashed lines) for a fluid particle as a function of the Lagrangian time starting at $t=0$ s with the shock, based on the free stream LTE conditions given in Table 1. Multi-temperature model using the Park (1993) rate coefficients for a 5-species mixture (N , N_2 , N^+ , N_2^+ and e^-) with standard mechanism (thick lines) and for a 2-species mixture (N and N_2) with simplified mechanism (thin lines).

Lagrangian time [s]	Distance from the shock [m]
0	0
10^{-14}	1.7×10^{-11}
10^{-13}	1.7×10^{-10}
10^{-12}	1.7×10^{-9}
10^{-11}	1.7×10^{-8}
10^{-10}	1.7×10^{-7}
10^{-9}	1.7×10^{-6}
10^{-8}	1.7×10^{-5}
10^{-7}	1.7×10^{-4}
10^{-6}	1.7×10^{-3}
10^{-5}	1.4×10^{-2}
10^{-4}	9.2×10^{-2}
10^{-3}	7.2×10^{-1}
10^{-2}	6.4

TABLE 2. Lagrangian time for a fluid particle and corresponding distance from the shock for the vibrational CR model.

population of the lowest energy levels, highly populated. Although described by different dynamics, the vibrational relaxation times for the two models, defined as the length of time required for thermalization among the vibrational and rotational-translational energy modes, are very similar. Thermalization is described differently by the two models: while the two-temperature model of Park predicts an overshoot for the vibrational temperature and a slow relaxation to equilibrium, the CR model allows for a chemistry-vibration coupling leading to a monotonic relaxation to equilibrium.

Figure 4 shows a slower dissociation rate for the Park model than for the CR model at the early stages of dissociation, whereas this trend is inverted at later stages. This behavior can be explained by a strong underprediction of the dissociation rate for large differences among the vibrational and translational temperatures.

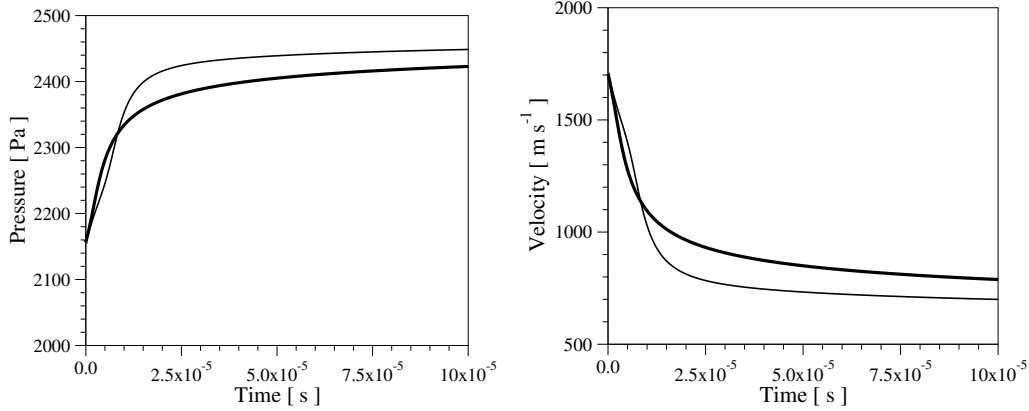


FIGURE 2. Post-shock pressure (*left*) and velocity field (*right*) for a fluid particle as a function of the distance from the shock, based on the free stream LTE conditions given in Table 1. Vibrational CR model (thick line) and multi-temperature model (thin line) for the 2-species mixture with simplified mechanism.

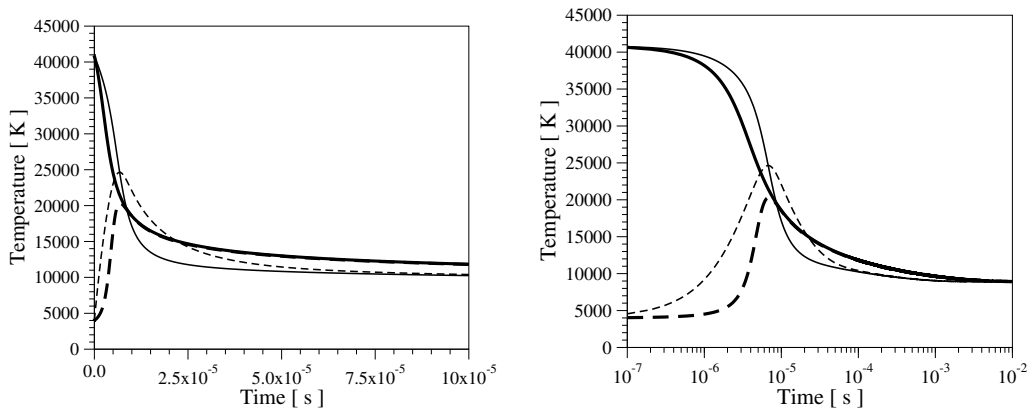


FIGURE 3. Post-shock translational temperature (unbroken lines) and vibrational temperature (dashed lines) for a fluid particle as a function of the Lagrangian time starting at $t=0$ s with the shock, based on the free stream LTE conditions given in Table 1. Vibrational CR model (thick lines) and multi-temperature model (thin lines) for the 2-species mixture with simplified mechanism. Left: linear time scale; right: logarithmic time scale.

Figure 5 shows the post-shock population for the vibrational energy levels of the nitrogen molecule in function of their vibrational energy, computed by means of the vibrational CR model. This figure clearly points out deviations from a Boltzmann distribution. As expected, the populations of the highest vibrational levels increase first, and, due to multi-quantum transitions, we notice the formation of a plateau for high vibrational states. The population density of this plateau increases with time up to $t = 10^{-6}$ s while the populations of the first vibrational levels remain unchanged. For $t > 10^{-6}$ s, a significant dissociation occurs and the population of all vibrational states decreases. Then, almost all the vibrational energy levels, except those very close to the dissociation energy, follow a Boltzmann distribution at a vibrational temperature that slowly converges toward 8900 K.

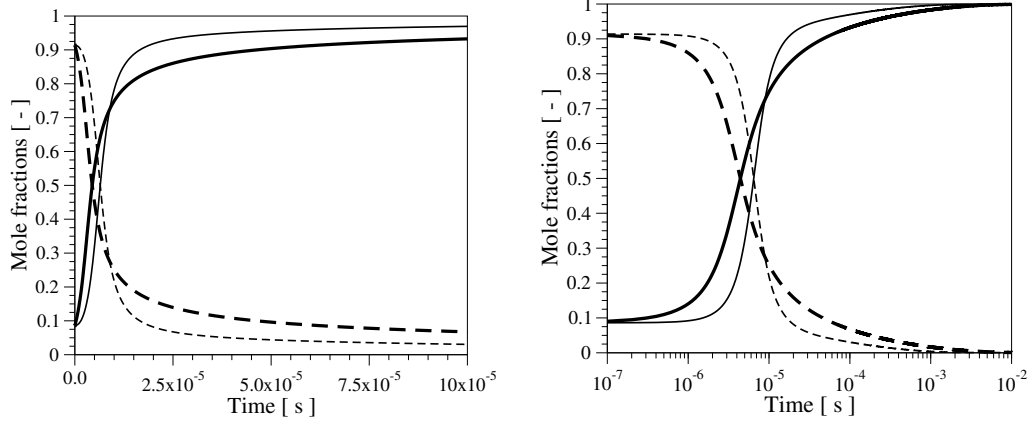


FIGURE 4. Post-shock nitrogen atom mole fraction (unbroken lines) and nitrogen molecule mole fraction (dashed lines) for a fluid particle as a function of the Lagrangian time starting at $t = 0$ s with the shock, based on the free stream LTE conditions given in Table 1. Vibrational CR model (thick lines) and multi-temperature model (thin lines) for the 2-species mixture with simplified mechanism. Left: linear time scale; right: logarithmic time scale.

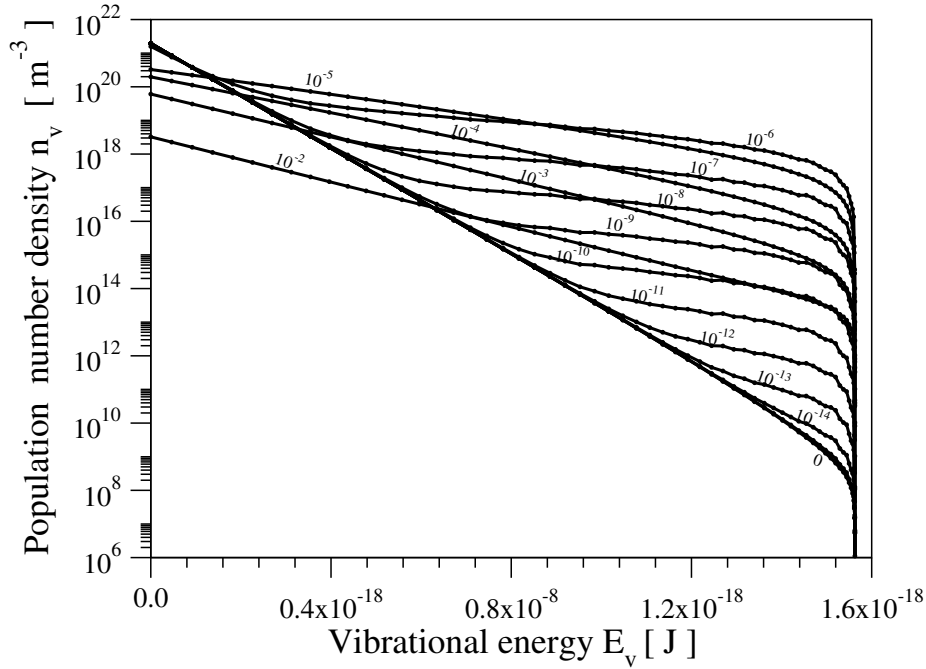


FIGURE 5. Post-shock population of the vibrational energy levels of the nitrogen molecule as a function of their vibrational energy for the Lagrangian times of a fluid particle, $t = 0, 10^{-14}, 10^{-13}, \dots, 10^{-3}, 10^{-2}$ s, obtained by means of the vibrational CR model based on the free stream LTE conditions given in Table 1.

4. Future plans

In this work, we have developed a 1D vibrational state-to-state model to describe the internal energy relaxation and dissociation processes behind a strong shockwave in a ni-

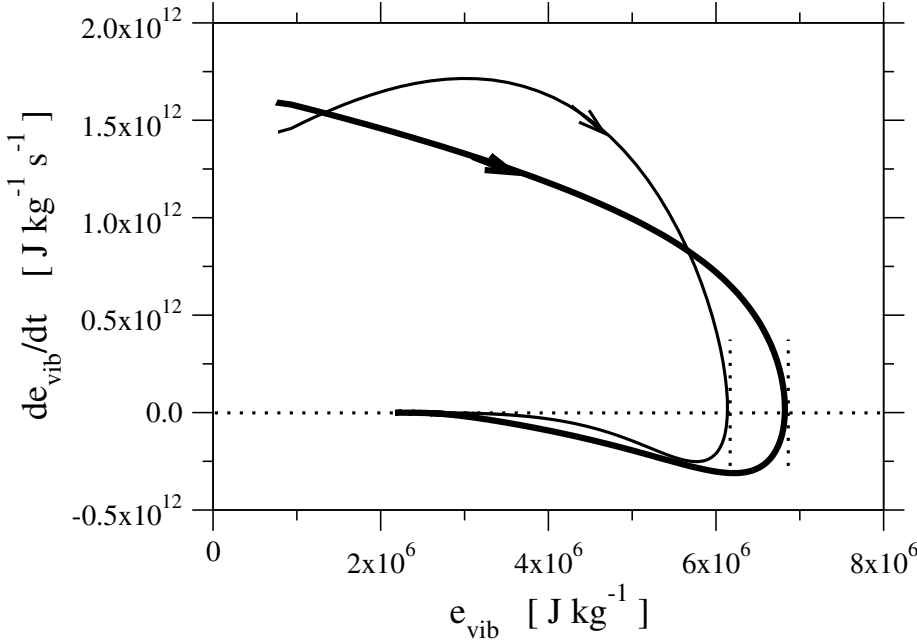


FIGURE 6. Post-shock vibrational energy trajectory in the phase space $(de_{vib}/dt, e_{vib})$ for a fluid particle, obtained by means of the vibrational CR model (thick line) and multi-temperature model (thin line) based on the free stream LTE conditions given in Table 1.

trogen flow. The 61 vibrational energy levels for the nitrogen molecule of the NASA Ames database were taken into account, as well as all the averaged elementary rate coefficients for excitation and dissociation, assuming that, for each vibrational level, the rotational energy level populations follow a Boltzmann distribution at the translational temperature. The results obtained were compared to the classical multi-temperature model proposed by Park and often used in the aerospace community for non-equilibrium flow simulations. We propose to use the CR model to determine a new macroscopic model of vibrational energy relaxation to be used in multi-temperature models, together with the corresponding chemistry-vibration coupling term. In a preliminary step, one can assess the validity of the Landau-Teller law widely used in multi-temperature models for non-equilibrium flow simulations. In Figure 6, the post-shock vibrational energy trajectory is shown in the phase space $(de_{vib}/dt, e_{vib})$ for a fluid particle. This vibrational energy is computed by means of Eq. (2.5) for the vibrational CR model, while it is computed by means of the vibrational temperature based on the assumption of a harmonic oscillator for the multi-temperature model. The vibrational dynamics described by means of the CR model is different from the dynamics described by means of the classical multi-temperature models. We also propose to develop a rovibrational collisional radiative model by relaxing the assumption of the Boltzmann distribution for the rotational energy levels. The energy levels will be lumped into bins as a function of their global internal energy, independently of their vibrational and rotational contributions.

Acknowledgments

The authors have benefitted from helpful discussions with Dr. G. Chaban and Dr. W. Huo at NASA Ames Research Center, Dr. A. Brandis at Stanford University, and Prof. C. Laux at Ecole Centrale Paris. The authors would like to thank Dr. N. Mansour and Dr. S. Yoon from NASA Ames Research Center.

REFERENCES

- APPLETON, J. P., STEINBERG, M. & LIQUORNIK, D. J. 1968 Shock-tube study of nitrogen dissociation using vacuum-ultraviolet light absorption. *Journal of Chemical Physics* **48** 599.
- BOURDON, A., PANESI, M., BRANDIS, A., MAGIN, T. E., CHABAN, G., HUO, W., JAFFE, R. & SCHWENKE D. W. 2008 Simulation of flows in shock-tube facilities by means of a detailed chemical mechanism for nitrogen excitation and dissociation, *Proceedings of the Summer Program 2008*, Center for Turbulence Research, Stanford University, NASA Ames Research Center.
- BULTEL, A., CHERON, B., BOURDON, A., MOTAPON, O. & SCHNEIDER, I. 2006 Collisional radiative model in air for Earth re-entry problems. *Physics of Plasmas* **13**(4) 11.
- CHABAN, G., JAFFE, R. , SCHWENKE, D. & HUO, W. 2008 Dissociation cross-sections and rate coefficients for nitrogen from accurate theoretical calculations. *AIAA 2008-1209, 46th AIAA Aerospace Sciences Meeting and Exhibit*, Reno, Nevada.
- ESPOSITO, F., ARMENISE, I. & CAPITELLI, M. 2006 N-N₂ state-to-state vibrational-relaxation and dissociation rate coefficients based on quasiclassical calculations. *Chemical Physics*, **331**(1) 1.
- JAFFE, R., SCHWENKE, D., CHABAN G. & HUO., W. 2008 Vibrational and rotational excitation and relaxation of nitrogen from accurate theoretical calculations. *AIAA 2008-1208, 46th AIAA Aerospace Sciences Meeting and Exhibit*, Reno, Nevada.
- JAFFE, R., SCHWENKE, D. & CHABAN G. 2009 Theoretical analysis of N₂ collisional dissociation and rotation-vibration energy transfer. *AIAA 2009-1569, 47th AIAA Aerospace Sciences Meeting and Exhibit*, Orlando, Florida.
- LAUX., C.O. 2002 Radiation and non-equilibrium collisional radiative models. *VKI-LS 2002-07, Physico-chemical models for high enthalpy and plasma flows*, Rhode-Saint-Genève, Belgium.
- MACHERET, S. O. AND ADAMOVICH, I. V. 2000 N-N₂ semiclassical Modeling of State-Specific Dissociation Rates in Diatomic Gases. *Chemical Physics*, **113**(17) 7351.
- MAGIN, T. E., CAILLAULT, L., BOURDON, A. & LAUX, C. O. 2006 Non-equilibrium radiative heat-flux modeling for the Huygens entry probe. *Journal of Geophysical Research - Planets*, **111** E07S12.
- PANESI, M., MAGIN, T., BOURDON, A., BULTEL, A. & CHAZOT, O. 2009 Analysis of the Fire II Flight experiment by means of a collisional radiative model, *Journal of Thermophysics and Heat Transfer*, **23** 236.
- PARK, C. 1990 *Non-equilibrium hypersonic aerothermodynamics*. Wiley, New York.
- PARK, C. 1993 Review of chemical-kinetic problems of future NASA mission, I: Earth entries. *Journal of Thermophysics and Heat Transfer*, **7**(3) 385.
- PARK, C. 2006 Thermochemical relaxation in shock-tubes. *Journal of Thermophysics and Heat Transfer*, **20**(4) 689.

- SCHWENKE, D. 1990 A theoretical prediction of hydrogen molecule dissociation-recombination rates including an accurate treatment of internal state non-equilibrium effects. *Journal of Chemical Physics*, **92** 7267.
- SCHWENKE, D. 2008 Dissociation cross-sections and rates for nitrogen. *VKI LS 2008, Non-equilibrium Gas Dynamics, from Physical Models to Hypersonic Flights*, Rhode-Saint-Genèse, Belgium.